A High Fidelity Computational Method for Flow-Tissue Interaction in Biological Flows

Xudong Zheng[1] and Rajat Mittal[2]

Department of Mechanical and Aerospace Engineering
The George Washington University, Washington, DC, 20052, U.S.A

Flow induced vibration and deformation are phenomena that routinely occur in biological systems including cardiovascular dynamics, phonation and biological locomotion, and computational modeling of such phenomena remains a challenge. The biophysics of phonation (which refers to the production of sound in the larynx) in particular is primarily driven by a highly coupled interaction between glottal aerodynamics and vocal fold tissue. In the current work, we have developed a coupled 3D immersed-boundary finite-element method (IBFEM) for modeling the interaction of fluid with biological structures (tissue) and applied this method to investigate the biophysics of phonation. In this method, the Navier-Stokes equations for fluid flow are solved using a sharp interface immersed boundary method (IBM). The elastrodynamic equations for the tissue are solved using a finite--element method which is coupled with the IBM solver. The results are analyzed to gain an insight into the glottal jet aerodynamics as well as the dynamics and deformation of the vocal folds. Results show that self--sustained vibrations can be achieved for the modeled vocal fold.

I. Introduction

PHONATION is a complex biological phenomenon which results from a highly coupled biomechanical interaction between glottal aerodynamics and vocal fold tissue vibration. The vocal folds are driven by transglottal pressure drop and vibrate mostly at a single frequency which is very close to one of the modal frequencies of the vocal folds. This frequency is the fundamental phonation frequency and decides the pitch of speech. Also a pulsatile transitional/turbulent jet is formed by the pressure drop and the moving wall of the vocal folds. The coupling of this jet with a very complicated human airway produces a complex flow field. The pulsatile jet flow and flow vortices are sound source and determine the voice quality.

Due to the high complexity of human airway lumen geometric shape and nonlinearity of the coupling between airway flow aerodynamics and vocal fold vibration, modeling this problem is an immense challenge. Early studies have employed the lumped mass vocal folds model coupled with the Bernoulli equation[5]. Despite its simplicity, these models were able to demonstrate sustained vocal fold vibration and pulsatile flows. However, lumped mass models cannot precisely predict continuum system behavior[8] and flow models based on the Bernoulli equation provide no information on development of the glottal jet. Hence more sophisticated models have been used for the airflow as well as the vocal fold modeling. The lumped model has been coupled with Naiver-Stokes equations[4]. The results show that the glottal jet has a strong asymmetry which also has been observed through experiments[6]. Furthermore, the continuum vocal fold has been coupled with steady Navier-Stokes equations in 3D elliptic cylinder type channel using finite element method[2].

In the current paper a new computational method for flow--structure interaction in biological flows is presented. The method employs a recently been developed sharp interface immersed boundary method (IBM)[1] for the fluid and a finite-element method (FEM) for the solid (tissue) dynamics. In addition, a penalty method is incorporated into the FEM to model the collision between solid structures. Two- and three--dimensional idealized geometric models are developed based on the shape of vocal folds obtained from real human larynx CT scans. The vocal fold tissue is modeled as a three-layer viscoelastic material. Two- and three-dimensional flow structure interaction (FSI) studies are conducted and results of these simulations presented.

[1] Ph.D. Candidate, AIAA Member.
[2]Professor, AIAA Associate Fellow. mittal@gwu.edu

II. Fluid-Structures Interaction Model of the Human Larynx

I. Glottal Flow Model

Glottal airflow during phonation is highly complex due to the inherent unsteadiness imposed by the vocal folds vibration as well as transition to turbulence in the glottal jet. The equations governing this type flows are the 3-D unsteady incompressible Navier--Stokes equations:

$$\frac{\partial u_i}{\partial x_i} = 0 \tag{1}$$

$$\frac{\partial u_i}{\partial t} + \frac{\partial u_i u_j}{\partial x_j} = -\frac{1}{\rho}\frac{\partial p}{\partial x_i} + \nu \frac{\partial^2 u_i}{\partial x_j \partial x_j} \tag{2}$$

where u_j are velocity components in three directions, p is pressure, and ρ and υ are flow density and kinematic viscosity

The equations are discretized in space using a cell--centered, non--staggered arrangement of the primitive variables u_i and p. A second--order fractional step method is used to integrate the equation in time. The advection term is linearized using a second--order Adams--Bashforth scheme. Also, an implicit Crank--Nicolson scheme is employed to discretize the diffusion term and to eliminate the viscous stability constraint. A line--SOR scheme is used to solve the advection--diffusion equation and an alternating--direction, geometric multi-grid with a line--SOR smoother is used to solve the pressure Poisson equation.

A sharp interface immersed boundary method (IBM) is used for solving these equations. Figure 1 shows a two--dimensional schematic of an immersed boundary on a Cartesian grid where the curve crossing the cells is the fluid--solid interface. Cells with a black circle at the center represent fluid cells, and those with a square represent solid cells. The value of the variables at the ghost cell (GC) is determined through extrapolation from image-point (IP) and boundary-intercept (BI). The sharp--interface boundary conditions are then imposed by involving the ghost cells in the computational molecule of the fluid cells in the vicinity of the sharp boundaries. Further details of this immersed boundary method can be found in Ref. [7].

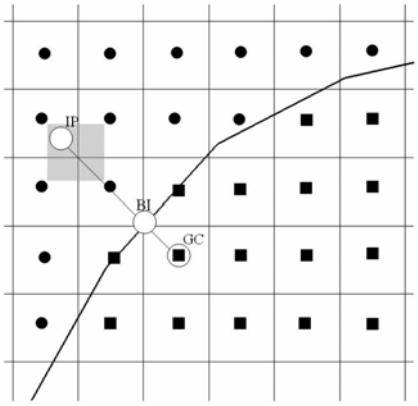

Figure 1. Schematic of ghost-cell methodology used in the current immersed boundary method.

II. Tissue Model

Just like other organs, the human vocal folds are made of different kinds soft tissues. From a biomechanics aspect, the vocal folds can be considered to be made of transverse isotropic viscoelastic materials. Since during normal phonation, vocal folds vibration causes small deformation, vocal folds are considered as linear viscoelastic material. The constitutive law for this type material is as follows[12]

$$\sigma_{ij} = C_{ijkl}\varepsilon_{kl} + A_{ijkl}\dot{\varepsilon}_{kl} \tag{3}$$

where σ is stress tensor, ε is train tensor, $\dot{\varepsilon}$ is strain rate tensor and *C* and *A* are four-order tensor of material constants.

The dynamics of continuum vocal folds are governed by the Navier equation.

$$\sigma_{ij,j} + \rho f_i = \rho \ddot{u}_i \tag{4}$$

where i and j range from 1 to 3, f_i is the body force component in i direction, ρ is vocal fold tissue density, u_i is displacement in i direction and $\ddot{u}_i$ is the acceleration component in i direction. This equation is solved by the finite element method (FEM). For governing equation, a weak form integration is used and in combination with the divergence theorem the resulting finite element equation is as follows:

$$M_{\alpha\beta}\ddot{U}_\beta + C_{\alpha\beta}\dot{U}_\beta + K_{\alpha\beta}U_\beta = F^\alpha \tag{5}$$

where M represents the mass matrix, C represents the damping matrix, K represents the stiffness matrix, F represents finite element nodal force and U represents the nodal displacement.

In order to model the vocal folds collision, the contact model based on penalty coefficient method has been integrated. The contact nodal force is modeled as follows:

$$F_{\alpha}^{contact} = \int_{\partial v^c} \varepsilon g \nabla g N_a da \tag{6}$$

where $F_{\alpha}^{contact}$ is the nodal contact force, ∂v^c is the contact area, ε is the penalty coefficient, g is the penetration distance, N_a is the shape function and a is the elementary area.

Eq.(5) is a second-order ordinary differential equation in time. It is discretized in time using the second order New-Mark scheme[12] wherein a banded LU decomposition is used to solve the system of algebraic equations. The Cuthill-McKee and Gibbs-Poole-Stockmeyer methods[13] are used to re-index the nodes in order to create banded matrixes.

III. Anatomical Model

Human vocal folds are located inside the larynx, just below the ventricle and between thyroid, cricoid and arytenoid cartilage. The shape of vocal folds and false vocal folds are reconstructed based on a high resolution CT scan. This CT scan is taken at The George Washington University hospital from a 30 years old normal male subject during phonation. A coronal view of larynx (located at l06.26*mm* from subject back) is used to create ideal human vocal folds and false vocal folds shape. Due to the slight rotation of subject's head, only the right part is used and left part is created by mirroring the right part from centerline. The ideal 2D/3D model is created by extruding the 2D model in anterior and posterior direction.

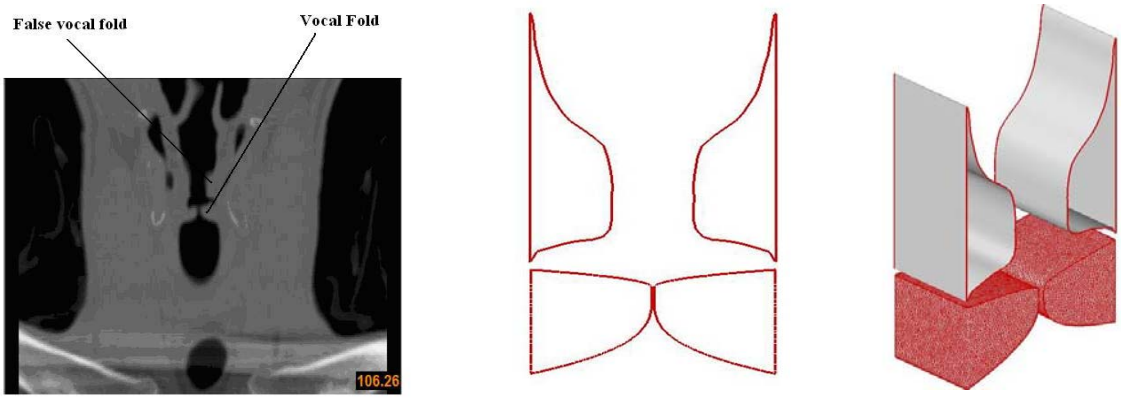

(a) **(b)** **(c)**

Figure 2. Vocal folds and false vocal folds anatomical model. (a) Coronal view of human larynx.(b) 2D vocal folds and false vocal folds shape extracted from CT scan.(c) 2D/3D vocal fold and false vocal folds model by extruding 2D model

The internal anatomical structure of vocal folds is made of different tissue layers. These layers (from superficial to deep) are cover, ligament and vocalis muscle. The material properties of these layers are shown in the Table 1 where ρ is the tissue density, E_p is the transversal Young's Modulus, ν_p is the in plane transversal ration, E_{pz} is the longitudinal Young's Modulus, ν_{pz} is the longitudinal Poisson's ratio, G_{pz} is the longitudinal shear modulus. Since during the normal phonation, the false vocals are hardly move. Here they are treated as rigid bodies.

Table 1. Material properties of the three-layers of the vocal folds

	$\rho(g/cm^3)$	$E_p(kPa)$	$E_p(kPa)$	$E_{pz}(kPa)$	ν_{pz}	$G_{pz}(kPa)$	$\eta(poise)$
cover	1.043	2.041	0.9	20	0.0	10	3
ligament	1.043	3.306	0.9	80	0.0	40	5
body	1.043	3.990	0.9	40	0.0	20	6

III. Simulation Results and Discussion

A. Eigen Mode Analysis

Eigen modes and eigen frequencies represent the possible responses of the structure to the external load. During the phonation, vocal folds typically vibrate at a single resonant frequency which is the fundamental phonation frequency. Despite the non-linearity in the fluid-tissue interaction, this resonant frequency is usually not far away from one of the vocal folds eigen frequencies. So eigen mode analysis can give good insight into the vocal fold vibration during phonation. Here both 2D and 3D eigen mode analysis have been performed. For 2D problem, it is assumed to be a plain isotropic strain problem which takes the same longitudinal shear modules with 3D case and a Poisson's ratio of 0.3. The first three lower eigen modes and eigen frequencies are shown in Figure 3. In the first mode, the vocal folds move in the inferior and superior direction whereas in the second mode that the vocal folds move in the medial and lateral direction, doing adduction and abduction. Finally, the third mode is that of a wave traveling along the vocal folds (the so called mucosal wave[11]).

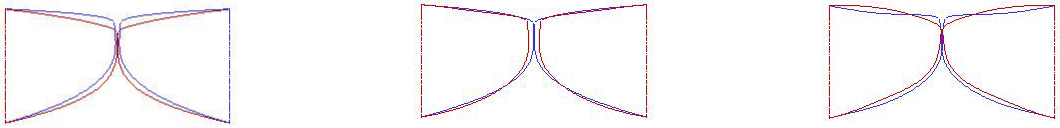

(a) Mode 1; 95.2Hz **(b)Mode 2; 215.3 Hz** **(c) Mode 3; 244.6 Hz**

Figure 3. Eigen modes and eigen frequencies of 2D vocal fold model.

For the 3D case, the shape of vocal folds is creating by extruding 2D model 2 cm in anterior and posterior directions and the vocal folds are subjected to zero displacement at the spanwise boundaries. The first 3D mode is similar to the first 2D eigen mode in that the vocal folds move in the inferior/superior direction. There is a standing wave along the longitudinal direction, and the length of vocal folds is half of this wave length. The second mode also involves inferior-superior motion although for this case, the longitudinal wave has a wave length equal to the length of vocal folds. Both the third and fourth modes are corresponding to the second and third models in the 2D vocal folds: ie. mode three is an adduction and abduction mode and mode four corresponds to a mucosal wave mode.

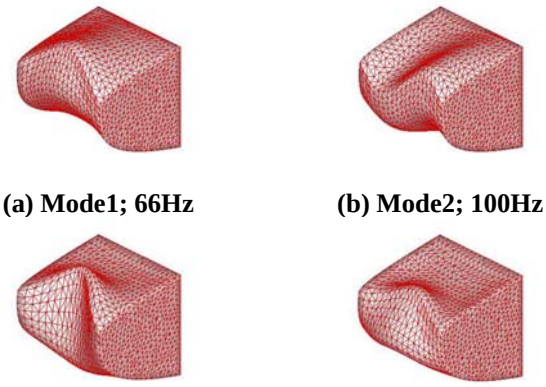

(a) Mode1; 66Hz **(b) Mode2; 100Hz**

(c) Mode 5; 109Hz **(d) Mode4; 125Hz**

Figure 4. Eigen modes and eigen frequencies of the 3D vocal fold model.

B. Fluid Tissue Interaction

1. Two-dimensional model of the Larynx

The 2D fluid tissue interaction simulation has been performed in a $12cm \times 2cm$ straight channel which represents the vocal tract in the vicinity of the larynx. The vocal folds extent from $x = 2.16cm$ to $x = 3.16cm$. The false vocal folds are downstream of the true vocal folds. The initial gap between the two vocal folds is 0.02cm. A constant pressure drop has been applied on the channel. The outlet pressure is chosen as reference pressure and the inlet gage pressure is $1\,kPa$. No penetration and no-slip boundary conditions are applied on the channel wall and fluid-tissue interfaces.

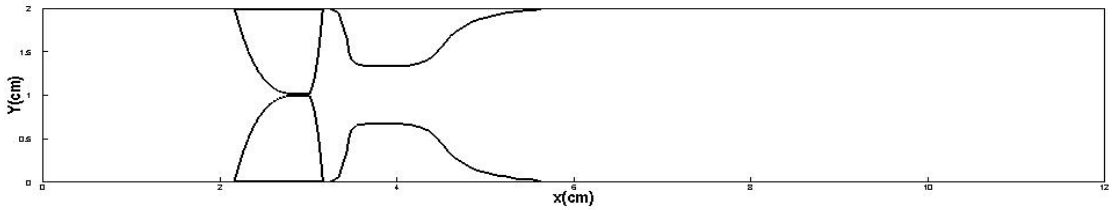

Figure 5. Flow domain for the 2D larynx model.

The flow simulation has been run on a non-uniform 288×256 Cartesian grid and the finite-element grid for the vocal fold structure has 117202 triangle elements. The simulation has been carried until it reaches a stationary state. Figure 6 shows the history of glottal gap width. It can be seen that at beginning, the vibration has several frequencies and after almost 10 cycles, the system seems to settle to a single frequency vibration. The average frequency over the steady cycles is 232*Hz*, which is between the second and the third eigen frequencies. The self-sustained vibration has been captured. Figure 7 shows the glottal width history from 0.17*s* to 0.185*s* for three cycles and it can be seen that the contact model works well in avoiding penetration between the two vocal folds.

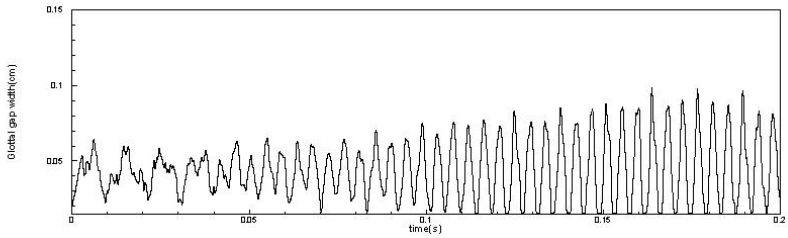

Figure 6. Time variation of the glottal gap width for the 2D larynx model.

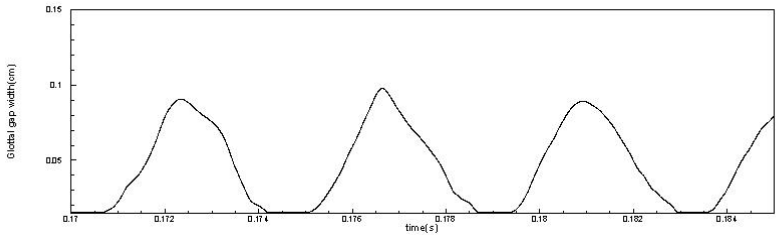

Figure 7. Time variation of the glottal gap width for 2D larynx model glottal width history from 0.17s to 0.185s

The instantaneous vorticity contours for one complete vibration cycle are shown in Figure 8. Results show that a pulsatile jet has been formed and this jet shows a strong asymmetry about the laryngeal centerline. It has been shown that for steady channel flow with a sudden expansion, the flow will become unstable and asymmetric beyond a critical Reynolds number even if the symmetric passage is provided, the total pressure drop due to vocal folds vibration.

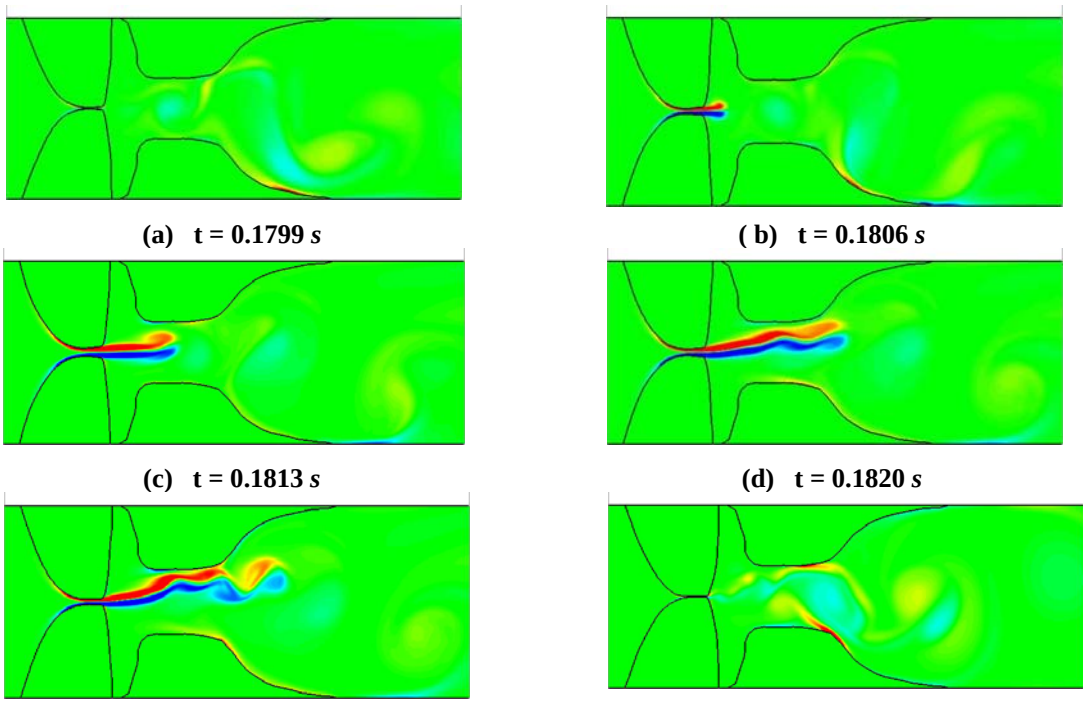

(a) t = 0.1799 *s* **(b) t = 0.1806 *s***

(c) t = 0.1813 *s* **(d) t = 0.1820 *s***

(e) t = 0.1824 *s* **(f) t = 0.1831 *s***

Figure 8. Instantaneous spanwise vorticity contours for one vocal fold vibration cycle.

Figure 9 shows contours of stress in the vocal folds during the maximum opening and closing phase. At the closing phase, the contact force produces a big compression stress (negative σ_y) on the medial surfaces of the vocal folds and the maximum elongation stress (positive σ_y) occurs at the root of ligament. The maximum shear stress τ_{xy} occurs on the root of vocal folds. At maximum opening position, the shear stress is much smaller than during the closing phase. The normal stress σ_y is mainly compressive during the opening phase and occurs at the superior part of the vocal fold body. The normal stress σ_x is similar at two position and is in general smaller than σ_y.

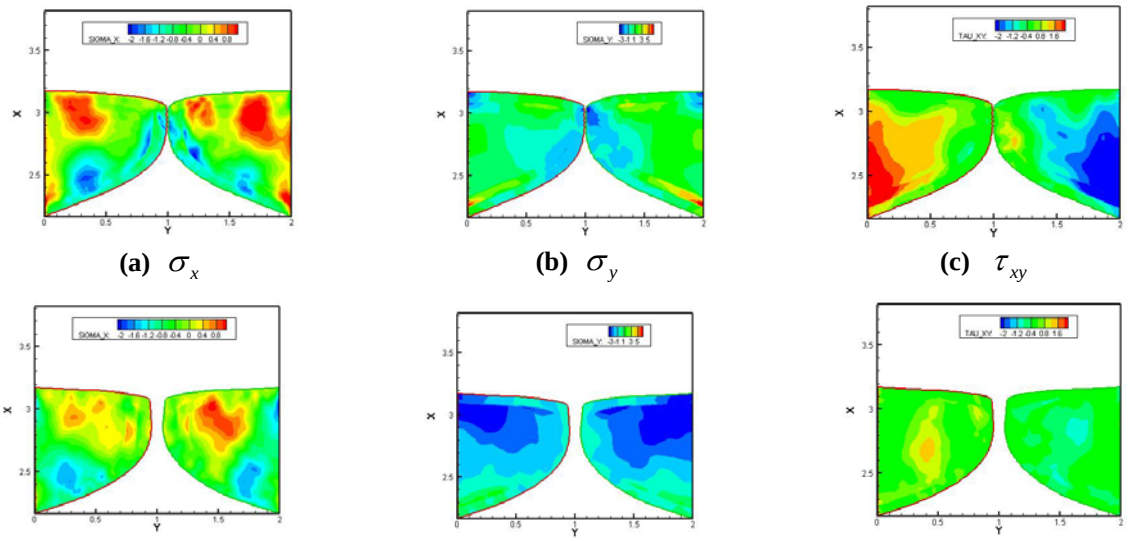

(a) σ_x **(b) σ_y** **(c) τ_{xy}**

(a) σ_x **(b) σ_y** **(c) τ_{xy}**

Figure 9. Contours of stresses in the vocal folds during the open and closed phase of the vibration cycle.

2. Three-dimensional Model of the Larynx

A $12cm \times 2.05cm \times 1.5cm$ straight rectangular duct has been used to mimic the human airway. For the true vocal folds, all of the surfaces except the flow tissue interfaces are fixed. All of the other conditions are similar to the 2D case. This simulation employs a nonuniform $128 \times 98 \times 64$ Cartesian grid for fluid solver and a 58427 tedrahedral element grid for the solid solver. The vortex structures at the closing and maximum opening phases are shown in Figure 10. The simulations indicate that the glottal jet is highly three-dimensional but despite the three-dimensionaly, shows a tendency to deflect towards one of the walls of the false vocal folds. Further simulations are exploring the three-dimensional nature of the jet and the vocal fold vibrations.

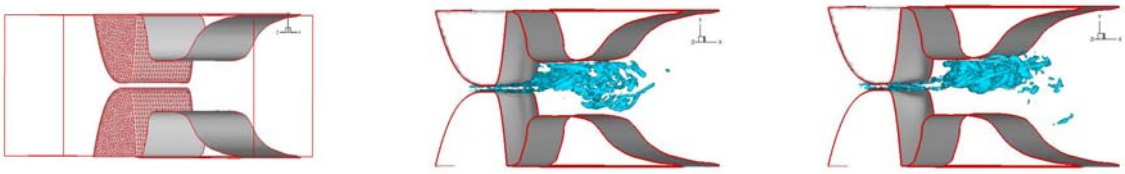

(a) **(b)** **(c)**

Figure 10. 3D FSI simulation setup and instantaneous vortex structure (a) grid used for true vocal folds in the 3D laryngeal model. (b-c) Vortex structures in the glottal jet at two instances in the vibration cycle.

Acknowledgments

The project described was supported by Grant Number ROlDC007125 from the National Institute On Deafness and Other Communication Disorders (NIDCD). The content is solely the responsibility of the authors and does not necessarily represent the official views of the NIDCD or the National Institutes of Health.

References

[1]Mittal, R. and Iaccarino G., "Immersed Boundary Methods," *Annu. Rev. Fluid Mech*., Vol.37, 2005, pp. 239-261.

[2]Rosa, M.O., and Pereira, J. C., "A Contribution to Simulating a Three-dimensional Larynx Model Using the Finite Element Method," *J. Acoust. Soc. Am.*, Vol. 114, No. 5, 2003, pp.2893-2905.

[3]Zhao, C., Zhao, W., Frankel, S.H., and Mongeau, L., "Computational Aeroacoustics of Phonation, Part I: Computational Methods and Sound Generation Mechanisms," *J. Acoust. Soc. Am*, Vol. 112, No.5, 2002, pp.2147-2154.

[4]Tao, C., Zhang, Y., Hottinger, G., and Jiang, J.J., "Asymmetric Airflow and Vibration Induced by the Coanda Effect in a Symmetric of the Vocal Folds," *J. Acoust. Soc. Am*, Vol. 122, No. 4, 2007, pp.2270-2278.

[5]Ishizaka, K., and Flanagan, J. L., "Synthesis of Voice Sound from a Two Mass Model of the Vocal Cords," *Bell System Tech. J.*, Vol. 51, 1972, pp.1233-1268.

[6]Neubauer, J., and Zhang, Z., "Coherent Structure of the Near Field Flow in a Self-oscillating Physical Model of the Vocal Folds," *J. Acoust. Soc. Am*, Vol. 121, No. ?, 2007, pp.1102-1110.

[7]Mittal, R., Dong, H., Bozkurttas, M., Najjar, F.M., Vargars, A. and Loebbecke, A.V., "A Versatile Sharp Interface Immersed Immersed Boundary Method for Incompressible Flows with Complex Boundaries," *J.Comput.*, Vol.227, 2008, pp. ?

[8]Alipour, F., Berry, D.A. and Titze, I.R.,"A Finite-element Model of Vocal-fold Vibration.," *J. Acoust. Soc. Am*, Vol. 108, No. 6, 2000, pp.3003-3012.

[9]Berg, V.D., Zantema, J.T. and Doornenbal, P., "On the Air Resistance and the Bernoulli Effect of the Human Larynx," *J. Acoust. Soc. Am*, Vol. 29, No. ?, 1952, pp.626-631

[10] Belyschko, T., Liu, W. and Moran, B., *Nonlinear Finite Elements for Consttinua and Structures*, 1st ed., JOHN WILEY and SONS LTD, New York, 2000.

[11] Ingo, R. T., *Principles of Voice Production*, 1st ed., PRENTICE HALL, Englewood Cliffs, New Jersey 1994.

[12] Robert, D. C., *Concepts and Applications of Finite Element Analysis*, 1st ed., JOHN WILEY and SONS LTD, New York, 1974.

[13]Everstine, G. C., "The Bandit computer program for the reduction of matrix bandwidth for Nastran," Technical Report 3827, David Taylor Naval Ship R&D Center, Bethesda MD, 1972.